Critical Flowmetering: The Characteristics of Cylindrical Nozzles with Sharp Upstream Edges

A. J. Ward-Smith*

A detailed study of the influence of axial length on the critical discharge coefficient of cylindrical orifices with sharp upstream edges is reported. Systematic consideration is given to the full range of geometries from the thin plate orifice up to the largest thickness/diameter (t/d) ratios of practical interest. A simple theoretical approach is used together with a more complete description of the physical nature of the flow. A range of orifice geometries is identified for which the critical discharge coefficient is independent of Reynolds number and t/d. Cylindrical nozzles in this range are particularly suited to critical flowmetering. They are simple to manufacture. Some new measurements are reported and these, together with existing experimental data, are shown to be consistent with the present analysis.

NOTATION

A	area
Cd^*	critical discharge coefficient
d	diameter of the orifice
f	friction factor for fully developed flow
$\bar{f}$	mean friction factor
K	coefficient defined by eq. (19)
L	distance from reattachment point to downstream extremity of nozzle
m	mass flow through the nozzle
M	Mach number
p	absolute pressure
P	pressure ratio, defined by eq. (2)
R	characteristic gas constant for air
t	nozzle thickness
T	absolute temperature
T_0	total temperature
u	mean velocity
α	value of t/d for marginally reattached incompressible flow
β	porosity coefficient $= A_2/A_1$
γ	ratio of specific heat capacities
δ	value of t/d below which choking corresponds with marginally reattached flow
ε	value of t/d for which area and Fanno choking occur simultaneously
ρ	fluid density
ϕ	contraction coefficient $= A_{3J}/A_2$
ϕ^*	value of ϕ under conditions of choking

Suffices

1	Condition in duct upstream of the nozzle
2	Condition at inlet plane of orifice
3	Condition in plane of maximum contraction of through-flow
4	Condition at plane of reattachment
5	Condition in exit plane of orifice
6	Condition in duct downstream of the nozzle
J	evaluated for the through-flow

* Lecturer in Mechanical Engineering, Brunel University, Uxbridge, Middx.

Received 6 March 1979 and accepted for publication on 25 July 1979.

INTRODUCTION

If the pressure downstream of a constriction in a gaseous flow is continuously reduced, whilst the conditions upstream are held constant, the flow rate increases until it eventually reaches a constant maximum value which cannot be exceeded by making further changes in the downstream pressure. The limitation of the mass flow rate in this way is known as choking and it is under these conditions of constant mass flow rate that critical or sonic flowmetering is employed.

In the simple one-dimensional model of compressible flow through a convergent-divergent nozzle (**1**), choking occurs when the flow becomes sonic at the plane of minimum cross-sectional area, the so-called throat. Due to the existence of regions of separation in the nozzles under consideration here, the flow is considerably more complicated. The occurrence of sonic conditions is a necessary condition for choking, but it is not a sufficient condition. This is because the geometry of the separated flow region can, under some circumstances, adjust in response to changes in downstream pressure.

When measuring low speed flows the plate orifice is the cheapest and most easily manufactured pressure differential device. However, this type of device is unsuitable for use as a critical flowmeter, due to the fact that the mass flow rate does not appear to reach a constant maximum value even when very small back pressure ratios are achieved.

Nozzles, venturi-nozzles, and short cylindrical orifices with appreciable rounding of the upstream edge, all of which preserve an attached flow between the upstream station and the downstream extremity of the throat, have been used for flow measurements at critical conditions. A disadvantage of these profiled nozzles is that they require a high standard of machining and in consequence are expensive to manufacture. Furthermore, they have been shown by Arnberg *et al.* (**2**) and others to be sensitive to Reynolds number effects, which are man-

0142/727X/79/0900-0123$02.00 © MEP Ltd 1979

ifested in a slight increase of discharge coefficient with increasing Reynolds number.

Measurements of the critical discharge coefficient for cylindrical sharp-edged nozzles of different thickness/diameter ratios have been reported in a number of papers (**3, 4, 5, 6, 7**). The performance of these nozzles has been shown (**3, 4**) to be insensitive to Reynolds number. There remain basic deficiencies in the understanding of the flow processes within the orifice and of the way the flow patterns are related to the discharge characteristics*. It is with these latter factors in particular that the present paper is concerned.

The work reported here examines the effects of axial length on the sonic flowmetering characteristics of nozzles with a circular-cylindrical bore. Systematic consideration will be given to the full range of geometries from the thin-plate orifice ($t/d \to 0$) up to the largest thickness/diameter ratios of practical interest. The work falls naturally into three parts. In the first a description of the general features of the flow is provided. Throughout the aim is to present as comprehensive a picture as possible consistent with current knowledge related to four basic points of reference. These are (1) the flow fields in these nozzles under conditions of incompressible flow (**8**), (2) information on the compressible flow in nozzles with separated flow ($t/d \to 0$) (**11, 12, 15, 16**), (3) the understanding of compressible flow phenomena in profiled nozzles with attached flow (**1**) and (4) experimental data on certain specific aspects of flow in cylindrical nozzles, e.g., flow visualization data (**9**) and measurements of pressure distribution (**5**). In the second part of the paper a simple theoretical analysis is derived, the aim of which is to predict the basic trends of the discharge characteristics of these nozzles as a function of t/d. Finally, in the third part of the paper these predictions are compared with experimental data.

This paper is concerned with high Reynolds number flow and porosity values near zero, i.e., the cross-sectional area of the orifice is small compared with the area of the approach flow. In these circumstances the geometry of the duct or environment into which the nozzle is set is of little importance in determining the flow properties of the nozzle.

The flow patterns which arise under conditions of incompressible flow will be briefly reviewed as they are closely related to the patterns which finally emerge when choking takes place. In all cases the fundamental feature of the flow is the separation initiated at the sharp upstream edge of the orifice. Although the boundary between the separated flow region and the main body of flow passing through the nozzle (which henceforth we shall refer to as the through-flow) is not well defined in regions subject to an adverse pressure gradient, due to the effects of turbulent mixing, for the sake of brevity the future discussions will proceed as though a distinct bounding streamline does exist.

The parameter of prime importance in determining the flow characteristics is the coefficient of contraction,

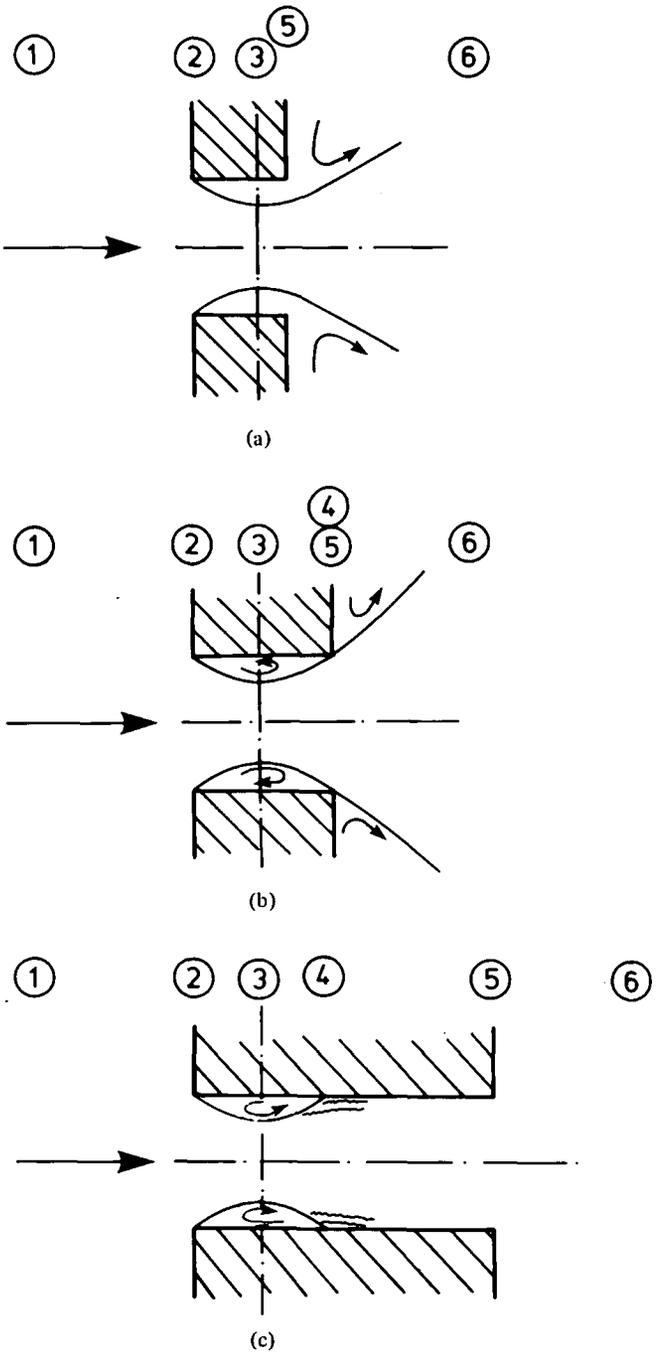

Fig. 1. Basic flow patterns under conditions of incompressible flow
(a) Separated flow; $0 < t/d < \alpha$
(b) Marginally reattached flow; $t/d \simeq \alpha$
(c) Fully reattached flow; $t/d > \alpha$

ϕ. This is the ratio between the minimum cross-sectional area occupied by the through-flow and the cross-sectional area of the orifice.

1 GENERAL FEATURES OF THE FLOW

1.1 Incompressible Flow Regimes

The fundamental feature of the incompressible flow at high Reynolds numbers in the nozzles under consideration is the separation of the flow from the sharp upstream edge of the orifice. The flow characteristics of the nozzle depend crucially on whether the free shear

* For example, Jackson (**5**) commented on his own results 'The variation of discharge coefficient with plate thickness is difficult to explain. One might have expected the discharge coefficient to fall with increasing plate thickness but this is not evident in the results'. The results presented in the present paper clearly explain the trends found by Jackson.

layer formed at the orifice entry remains separated or whether reattachment occurs within the orifice. Several different flow regimes have been identified and these are described in (**8**), to which the reader is referred for a fuller treatment. The three main types of flow pattern are depicted schematically in Fig. 1.

Separated Flow ($0 < t/d < \alpha$)

For small length to diameter ratios the flow separates away from the surface of the orifice and forms a discrete jet which contracts to a minimum cross-sectional area, at the vena contracta, together with a separated flow region between the jet and the orifice wall (as shown in Fig. 1a). Typically, this flow pattern occurs in the range $0 < t/d < \alpha$ where $\alpha \approx 0{\cdot}75$. In this range, ϕ increases monotonically from a value of $\phi = 0{\cdot}61$ at $t/d = 0$ to $\phi \approx 0{\cdot}8$ for $t/d = \alpha$.

Reattached Flow ($t/d \geqslant \alpha$)

Marginally Reattached

In this flow regime the flow just reattaches itself to the downstream edge of the orifice and immediately separates again. Theoretical considerations (**8**), indicate that this condition, which is a highly stable flow configuration, occurs over a small but finite range of t/d values near $t/d = \alpha$.

Fully Reattached Flow

The flow separates from the orifice leading edge and forms a free shear layer. At high Reynolds numbers transition takes place within the shear layer and reattachment occurs in the form of a turbulent boundary layer, resulting in a separation bubble being entrapped at the orifice entry. Downstream from the reattachment point the boundary layer develops and eventually separates at the downstream edge of the orifice. For orifices with reattached flow the geometry of the separation bubble is essentially independent of t/d. This flow regime occurs for values of $t/d > \alpha$ and in this range ϕ is constant at a value of about 0·61.

1.2 Compressible Flow Regimes Prior to Choking

A strong correlation exists between the performance of orifices with sharp upstream edges under conditions of compressible flow prior to choking and the flow regimes which occur in incompressible flow.

At the high Reynolds numbers under consideration the geometry of the separating flow pattern, and in particular the value of ϕ, is essentially unaffected by the Reynolds number.

For all values of t/d, as the back pressure ratio, p_6/p_1, is decreased from the incompressible limit, the mass flow rate and the Mach number at the vena contracta plane both increase. A change to the geometry of the flow pattern also occurs. The area of the vena contracta increases and there is a tendency for the through-flow to occupy a greater proportion of the flow field at the expense of the separated flow. There is a considerable body of evidence of this effect. For thin plate orifices ($t/d \to 0$) these trends have been shown experimentally (**10**) and theoretically (**11**, **12**). Related calculations for two dimensional flow fields also show similar trends. For orifices with reattached flow ($t/d > \delta$), the Schlieren photographs reported in (**9**) indicate that the size of the separation bubble for fully-reattached compressible flow

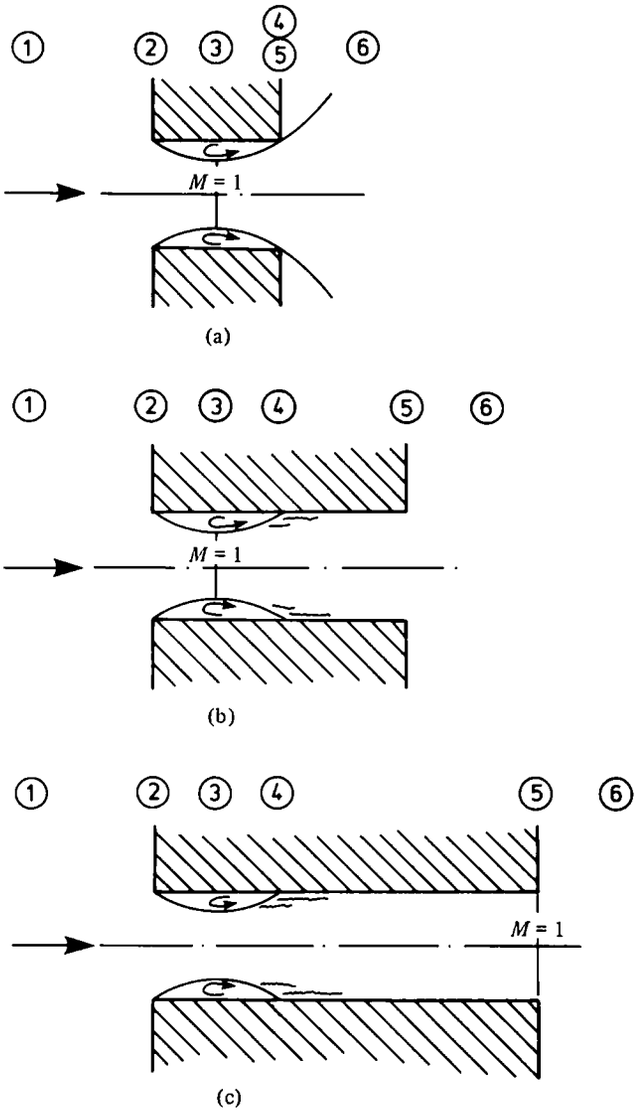

Fig. 2. Basic flow patterns when the flow first approaches the choked condition
(a) Marginally reattached flow; $0 < t/d < \delta$
(b) Fully reattached flow; $\delta < t/d < \varepsilon$
(c) Fully reattached flow; $t/d > \varepsilon$

is much smaller than would be expected at the incompressible limit.

These changes to the geometry of the flow pattern continue to occur as p_6/p_1 is reduced, until at some stage a stable pattern arises. There are three quite distinct ways in which this condition may be achieved, as Fig. 2 shows.

Marginally Reattached Flow ($0 < t/d < \delta$)

Under conditions of incompressible flow, nozzles in the range $0 < t/d < \delta$ give rise to a separated flow pattern. With decreasing p_6/p_1 the flow rate increases until the velocity in the through-flow at the vena contracta becomes sonic, the flow remaining separated from the orifice.

In a meter with attached flow, the presence of a sonic surface in the throat is equivalent to a physical barrier, because the effects of changes that are made downstream of this surface cannot be propagated upstream. Hence at

this condition the venturi tube and similar devices choke.*

In the nozzles under consideration, the sonic surface at the vena contracta does not prevent changes in p_6 affecting the shape of the bounding streamline upstream. And so further reduction in p_6/p_1 results in a more pronounced increase in the area of the vena contracta and a simultaneous movement of the vena contracta plane upstream. At sufficiently small pressure ratios, the area of maximum contraction approaches the upstream edge of the orifice and the jet just reattaches itself to the downstream edge of the orifice, before immediately separating again and expanding to downstream conditions. This is the final stage just prior to the onset of choking. The flow pattern now corresponds to marginally reattached flow, as depicted in Fig. 2(a).

Fully Reattached Flow ($\delta < t/d < \varepsilon$)

Nozzles in this range of geometries exhibit a fully reattached flow pattern as the choked condition is approached. The choked condition is achieved when the velocity in the plane of the vena contracta becomes sonic (Fig. 2b).

For nozzles in the range $\delta < t/d < \alpha$, as p_6/p_1 is reduced so the flow pattern in the nozzle changes at some stage from a separated to a reattached condition. Deckker and Chang (**4**) and Brain and Reid (**3**) report experimental observations on nozzles with $t/d \approx 0{\cdot}5$ which clearly demonstrate the existence of hysteresis effects, the nozzle displaying different discharge characteristics depending upon whether the back pressure is increased or decreased. These data provide important evidence of the flow pattern changing from the separated to the marginally reattached state, and vice versa. For a detailed explanation of this phenomenon the reader is referred to Ward Smith (**8**). From these data it can be inferred that $\delta < 0{\cdot}5$.

For nozzles in the range $\alpha < t/d < \varepsilon$ the flow remains reattached at all back pressure ratios from the incompressible limit through to the onset of choking.

Fully Reattached Flow ($t/d > \varepsilon$)

Up to this stage all of the nozzles discussed have choked when a Mach number of unity has been achieved at the vena contracta plane. With $t/d > \delta$ since part of the nozzle is subject to the frictional effects of a developing boundary layer, a different mechanism of choking becomes a possibility. Fanno choking occurs under conditions of adiabatic frictional flow in a duct of constant cross-sectional area when the Mach number at the downstream exit plane of the duct becomes equal to unity (**1**).

There is a particular nozzle geometry, denoted by $t/d = \varepsilon$ for which, with decreasing back pressure ratio, a Mach number of unity will occur simultaneously at the vena contracta plane and at the outlet plane of the nozzle. The flow rate is limited by Fanno choking in nozzles for which $t/d > \varepsilon$ as is shown schematically in Fig. 2(c).

1.3 The Choked Nozzle

It is now time to consider the fluid flow in the various geometries of nozzle when they become choked. Initially it is convenient to envisage the curved boundary of the entrapped separation bubble to be replaced by a corresponding fixed wall. The marginally reattached flow pattern then corresponds to flow through a convergent-divergent nozzle. For values of $t/d > \delta$, the orifice can be viewed as a parallel duct with friction, fed by a convergent-divergent nozzle at entry.

A brief description of the processes in the nozzles under conditions of choking is appropriate.

The simplest situation occurs for $t/d > \varepsilon$. When choking is initiated (Fig. 2(c)), the flow through the entire orifice is subsonic, except at the exit plane where the flow is sonic. Reduction of the back pressure below that corresponding to Fig. 2(c) results in the formation of an expansion wave system outside the nozzle exit, the flow within the orifice remaining unchanged.

For $0 < t/d < \varepsilon$ the situation is more complicated. The compressible flow regimes for one-dimensional adiabatic flow in convergent-divergent nozzles (see e.g. Chapter 5 of (**1**)) and for Fanno flow (see e.g. Chapter 6 of (**1**)) are well documented and it is an obvious step to seek to explain the phenomena in nozzles in the range $0 < t/d < \varepsilon$, as the back pressure is reduced below that corresponding to Fig. 2(a) and 2(b), by reference to these one-dimensional models. For nozzles in the range $0 < t/d < \delta$ this procedure is acceptable but for the range $\delta < t/d < \varepsilon$ the one-dimensional model provides an imperfect representation of the flow processes within the nozzles under consideration, as is confirmed by the flow visualization studies reported by Weir *et al.* (**9**). These results clearly show the oblique shock-wave patterns which occur within two-dimensional nozzles over a wide range of back pressure ratios, results which are inconsistent with a one-dimensional model.

The following description seeks to account for the more important details of the actual situation. Reduction of the back pressure, p_6, below that corresponding to Fig. 2(a) or 2(b) results initially in the formation of a weak normal shock wave at the plane of maximum contraction, plane 3. As the value of p_6 is progressively reduced the shock becomes stronger and travels downstream towards plane 4.

Due in part to viscous effects and, perhaps more importantly, to streamline curvature effects the compression shock will in practice differ from the plane discontinuity of one-dimensional flow theory. In particular, for $\delta < t/d < \varepsilon$, the region where the free shear layer reattaches to the wall of the orifice is, so far as the through-flow is concerned, effectively a concave corner, and once supersonic flow has been established between planes 3 and 4 it is from this locality that an oblique shock originates, giving rise to an oblique shock pattern downstream.

Whilst the shock stands in the region between the plane of maximum contraction, plane 3, and the reattachment plane 4, there exists the possibility of the shock modifying the geometry of the separation bubble. Only when a region of supersonic shock-free flow is estab-

* In principle the downstream effects can be propagated upstream in venturi-tubes, nozzles etc. in the slow moving stream tubes in the boundary layer. This effect would be manifested by a slow, creeping increase of m as p_6/p_1 was reduced below the critical value. There is no evidence that this effect is of any practical significance. The existence of such evidence would render critical flowmetering impractical.

lished between planes 3 and 4 will the geometry of the separation bubble remain quite independent of the processes downstream and therefore it is only when this stage is reached that nozzles in the range $0 < t/d < \delta$ can finally be regarded as choked.

It is worth drawing special attention to a feature of the flow in nozzles satisfying the condition $\delta < t/d < \varepsilon$. Once supersonic conditions have been established downstream of the reattachment plane in these nozzles, the downstream conditions cannot influence the geometry of the separation bubble at the orifice entry. At the choked condition, therefore, all of these nozzles will have a separated flow pattern which is identical and is therefore entirely independent of t/d. This feature has a fundamental effect on the critical discharge coefficient of these nozzles, with important practical consequences.

2 THEORETICAL ANALYSIS

2.1 Definition of the Critical Discharge Coefficient, Cd^*

The critical discharge coefficient will be defined as

$$Cd^* = \frac{m}{A_2 \left\{ \frac{2\gamma}{(\gamma-1)} p_1 \rho_1 P^{2/\gamma} \frac{(1 - P^{(\gamma-1)/\gamma})}{(1 - \beta^2 P^{2/\gamma})} \right\}^{1/2}} \quad (1)$$

where P is the pressure ratio given by the solution of the equation

$$2 - (\gamma + 1)P^{(\gamma-1)/\gamma} + \beta^2(\gamma - 1)P^{(\gamma+1)/\gamma} = 0 \quad (2)$$

The denominator of eq. (1) is often referred to loosely as the 'theoretical mass flow' at choking, since it is the mass flow rate derived using one-dimensional isentropic flow theory in a convergent-divergent nozzle with attached flow.

For the condition $\beta \to 0$

$$P \approx \left(\frac{2}{\gamma + 1} \right)^{\gamma/(\gamma-1)} \quad (3)$$

and the definition of the critical discharge coefficient simplifies to

$$Cd^* = \frac{m}{A_2(p_1\rho_1)^{1/2}} \frac{1}{\sqrt{\gamma}} \left(\frac{\gamma + 1}{2} \right)^{(\gamma+1)/2(\gamma-1)} \quad (4)$$

2.2 Theoretical Evaluation of The Critical Discharge Coefficient

The following general assumptions will be made in the analysis.

(1) The flow is that of a compressible perfect gas
(2) The properties of the flow at stations 1 and 6 and of the through-flow at station 3 may be adequately described by one-dimensional flow relations.
(3) (a) The flow between stations 1 and 3 is assumed isentropic. The favourable pressure gradient in this region justifies this assumption.
    (b) For $t/d = \varepsilon$ the flow between stations 4 and 5 is Fanno flow, i.e. compressible adiabatic frictional flow without area change.
(4) The mean static pressures of the separated flow and of the through-flow at station 3 are equal.

Incorporating the assumptions outlined above, the following equations may be set down for all of the configurations depicted in Fig. 2 when the flow becomes choked.

The energy equation applied to the main body of flow passing through the nozzle is

$$p_1 \left\{ 1 + \frac{\gamma - 1}{2} M_1^2 \right\}^{\gamma/(\gamma-1)} = p_{3J} \left\{ 1 + \frac{\gamma - 1}{2} M_{3J}^2 \right\}^{\gamma/(\gamma-1)} \quad (5)$$

The continuity equation is

$$m = \rho_1 A_1 u_1 = \rho_3 A_{3J} u_{3J} = \rho_4 A_4 u_4 \quad (6)$$

The equation of state is

$$p = \rho RT \quad (7)$$

The general definition of the coefficient of contraction is

$$\phi = A_{3J}/A_2 \quad (8)$$

We shall use the symbol ϕ^* to denote the particular value of ϕ corresponding to choking in the nozzle.

The porosity β is given by

$$\beta = A_2/A_1 \quad (9)$$

The definition of Mach number is

$$M = \frac{u}{a} = \frac{u}{\sqrt{(\gamma RT)}} \quad (10)$$

Combination of the above equations and substitution of the limit $\beta \to 0$ yields the resulting relation for the mass flow when the nozzle chokes as

$$m = \phi^* A_2 (p_1\rho_1)^{1/2} \frac{\sqrt{\gamma}\, M_{3J}}{\left\{ 1 + \frac{\gamma - 1}{2} M_{3J}^2 \right\}^{(\gamma+1)/2(\gamma-1)}} \quad (11)$$

Comparison of eqs. (4) and (11) yields the value of the critical discharge coefficient for the model analysed as

$$Cd^* = \phi^* M_{3J} \left\{ \frac{\gamma + 1}{2\left(1 + \frac{\gamma - 1}{2} M_{3J}^2 \right)} \right\}^{(\gamma+1)/2(\gamma-1)} \quad (12)$$

2.3 Variation of Cd^* with t/d

For nozzles in the range $0 < t/d < \varepsilon$ choking occurs when $M_{3J} = 1$ and so for this range of geometries the critical discharge coefficient is given by the simple relation

$$Cd^* = \phi^* \quad (13)$$

Since ϕ^* is independent of t/d for nozzles in the range $\delta < t/d < \varepsilon$, eq. (13) points to the important result that nozzles in this t/d range will have the same value of Cd^*. Following the discussions in Sections 1.2 and 1.3, for nozzles in the range $0 < t/d < \delta$, a decrease of Cd^* with increasing t/d is predicted.

For nozzles satisfying the condition $t/d > \varepsilon$, the Mach number in the through-flow at plane 3 is subsonic and so for these nozzles subject to Fanno choking it follows from eq. (12) that

$$Cd^* < \phi^*$$

In this range, a decrease of Cd^* with increasing t/d is

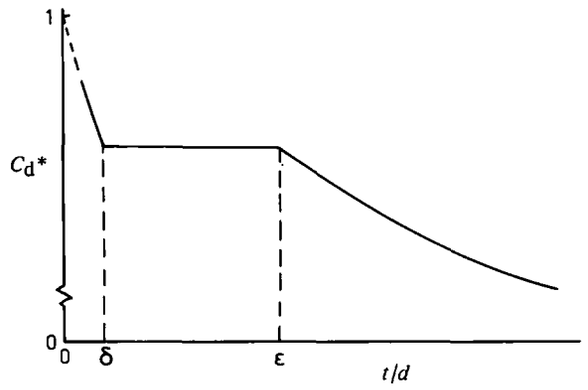

Fig. 3. Predicted trend of Cd^* with t/d

predicted. Since the magnitude of M_{3J} depends on the frictional characteristics of the flow between planes 4 and 5, the value of Cd^* will in general vary with Reynolds number and surface roughness.

The above predictions are summarized qualitatively in Fig. 3.

2.4 Theoretical Evaluation of ε

Using the assumptions set out in Section 2.2 and applying them to the model illustrated in Fig. 2(c) the following equations may be derived.

Applying a momentum balance between stations 3 and 4 there results

$$p_3 + \phi^* \rho_3 u_{3J}^2 = p_4 + \rho_4 u_4^2 \tag{14}$$

which can be rewritten as

$$p_3(1 + \phi^* \gamma M_{3J}^2) = p_4(1 + \gamma M_4^2) \tag{15}$$

Combination of the energy, state, and continuity equations locally within the flow yields the relation between the mass flow function and Mach number.

$$\frac{m\sqrt{(RT_0)}}{Ap} = \sqrt{\gamma}\, M \left\{1 + \frac{\gamma - 1}{2} M^2\right\}^{1/2} \tag{16}$$

Hence

$$\frac{p_4}{p_3} = \frac{\phi^* M_{3J}}{M_4} \left\{ \frac{1 + \frac{\gamma - 1}{2} M_{3J}^2}{1 + \frac{\gamma - 1}{2} M_4^2} \right\}^{1/2} \tag{17}$$

The ratio p_4/p_3 can be eliminated between eqs. (15) and (17) which, since $M_{3J} = 1$, leaves a relationship between ϕ^* and M_4.

Denoting the distance between stations 4 and 5 by L, the Fanno flow relations (1) can be used to determine L. Since $M_5 = 1$ these relations yield

$$\frac{4\bar{f}L}{d} = \frac{1 - M_4^2}{\gamma M_4^2} + \frac{\gamma + 1}{2\gamma} \log_e \left\{ \frac{(\gamma + 1) M_4^2}{2\left\{1 + \frac{\gamma - 1}{2} M_4^2\right\}} \right\} = \psi(M) \tag{18}$$

Because $Cd^* = \phi^*$ when $t/d = \varepsilon$, eq. (18) is a relationship between Cd^* and $4\bar{f}L/d$. This is plotted in Fig. 4 for a range of values of Cd^*.

In fully-developed flow, the friction factor f is a function of Reynolds number and relative roughness, but experiments show it to be independent of Mach number. Typical values of Reynolds numbers in the orifice flow under consideration are about 10^5.

The mean friction-factor of a developing boundary layer, $\bar{f}$, exceeds the friction factor for fully-developed flow, f. An assessment of the magnitudes involved can be made from the data for incompressible flow reported by Barbin and Jones (13).

The relation can be written as

$$\bar{f} = Kf \tag{19}$$

where K is a factor, typically in the range $1 < K < 1{\cdot}5$, which is itself a function of L/d. As $L/d \to \infty$, $K \to 1$.

Since ε is given by the approximate relation

$$\varepsilon = \delta + \frac{L}{d} \tag{20}$$

we have the final relation, obtained by combining eqs. (18)–(20)

$$\varepsilon = \delta + \frac{\psi}{4Kf} \tag{21}$$

Obviously ε will vary appreciably, due to the dependence of f on Reynolds number and, especially, relative roughness.

3 COMPARISON OF THEORY WITH EXPERIMENTAL RESULTS

3.1 Comparison of Theory with Published Data

For nozzles with knife-edge orifices, $t/d \to 0$, reattachment of the flow corresponds with the condition $\phi^* \to 1$. The theory of Section 2 therefore indicates that for choking to occur in knife-edged orifices the critical discharge coefficient must approach a value of unity. The highest value of discharge coefficient which has been measured (4), (5) in such nozzles is about 0·9, and during the entire course of these tests the flow rate increased with decreasing p_6/p_1. The smallest value of t/d tested by Brain and Reid (3) was 0·14 and again for values of p_6/p_1 as low as 0·2 the flow rate continued to increase with decreasing p_6/p_1. These results indicate that for practical purposes choking does not occur in nozzles with these small values of t/d. Brain and Reid (3) have shown that a nozzle with $t/d = 0{\cdot}28$ chokes at a value of $p_6/p_1 \approx 0{\cdot}38$.

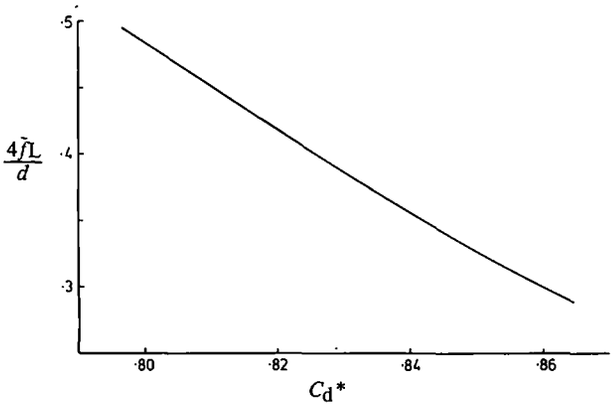

Fig. 4. Variation of $4\bar{f}L/d$ with Cd^*

Table 1

Critical discharge coefficients

Reference	t/d	Cd^*	Nozzle No.	Data Source*
3	0·14	†	8	F
	0·28	0·841	8	T
	0·31	0·83	5	F
	0·488	0·844	3	T
	0·50	0·83	7	F
	0·51	0·83	5	F
	0·51	0·839	6	T
	0·54	0·845	4	F
	0·92	0·825	7	F
	0·986	0·835	9	T
	1·01	0·83	2	F
	1·01	0·83	5	F
	1·02	0·845	4	F
	1·933	0·820	7	T
	1·97	0·825	2	T
	2·00	0·841	4	T
	2·00	0·832	5	T
	2·07	0·843	1	T
	3·48	0·839	4	T
	4·92	0·826	2	T
	5·13	0·842	1	T
4	2	0·86	—	F
	1	0·86	—	F
	0·5	0·88	—	F
	0	†	—	F
5	0·053	†	—	F
	0·33	0·845	—	F
	0·67	0·86	—	F
	1·0	0·835	—	F
	5·3	0·84	—	F
	10·62	0·82	—	F
6	1·00	0·83	—	F
7	1·45	0·830	—	T
	1·473	0·832	—	T
	1·476	0·840	—	T
	1·433	0·832	—	T
	1·453	0·829	—	T
14	4·00	0·85	—	F
	2·83	0·86	—	F
	2·00	0·86	—	F

* T = tabulated. F = figure.
† Nozzle did not choke.

At higher values of t/d, choking has consistently been found to occur, and the values of Cd^* measured by different authors are given in Table 1. The work of Brain and Reid (**3**) is particularly helpful. Apart from the nozzle which did not choke, they tested geometries in the range $0{\cdot}28 < t/d < 5{\cdot}13$ and measured values of critical discharge coefficient in the range $0{\cdot}82 < Cd^* < 0{\cdot}845$. Brain and Reid made a number of tests in which they took the same basic nozzle and sliced away the downstream face in order to alter the t/d ratio. This process did not alter the value of Cd^* for the nozzle (see Table 1), a result which is in exact agreement with the theoretical prediction of Section 2, namely that Cd^* is independent of t/d in the range $\delta < t/d < \varepsilon$. On the other hand, the results of Brain and Reid show that for different nozzles with nominally the same value of t/d, there is a small amount of scatter in Cd^*, which is probably due to very slight differences in the geometry of the leading edge between one nozzle and another, or due to small inaccuracies in the measurement of d. Comparing the results from the different sources as a whole (Fig. 5 and Table 1) a scatter of about $\pm 2{\cdot}5$ per cent about the mean is observed. In part the scatter is due to experimental errors of the type just discussed, but it has been exacerbated in some cases where data have been read from diagrams and the scale did not provide the desired level of accuracy. The latter is indicated in Table 1 by the symbol *F*. The 26 data points of Table 1 in the range $0{\cdot}75 < t/d < 10$ are correlated by the relation $Cd^* = 0{\cdot}838$ with a standard deviation of 0·011 5.

The significance of the invariance of Cd^* with t/d under conditions of compressible flow for nozzles in the range $\delta < t/d < \varepsilon$ is highlighted by the corresponding curves for incompressible flow which are plotted on Fig. 5. These lines represent the correlation of experimental data from numerous sources reported in (**8**). Above a value of $t/d = 3$ the effect of friction causes a systematic reduction of the incompressible discharge coefficient, Cd, with increasing t/d, where Cd is defined by

$$Cd = \frac{m}{A_2(p_1 - p_6)\rho_1^{1/2}} \frac{1}{(1-\beta^2)^{1/2}}$$

It is now appropriate to discuss the experimental evidence relating to the magnitudes of δ and ε. So far as δ is concerned, we have suggested in Section 2 that $\delta < 0{\cdot}5$. The tests on nozzle 5 reported by Brain and Reid would seem to indicate that $\delta < 0{\cdot}3$. There are no further results from which a more definite magnitude can be obtained. As t/d is reduced below $t/d = 0{\cdot}3$, the situation is soon reached where the nozzle does not choke and so, on this evidence, a value of $\delta = 0{\cdot}3$ may be viewed as a useful working approximation.

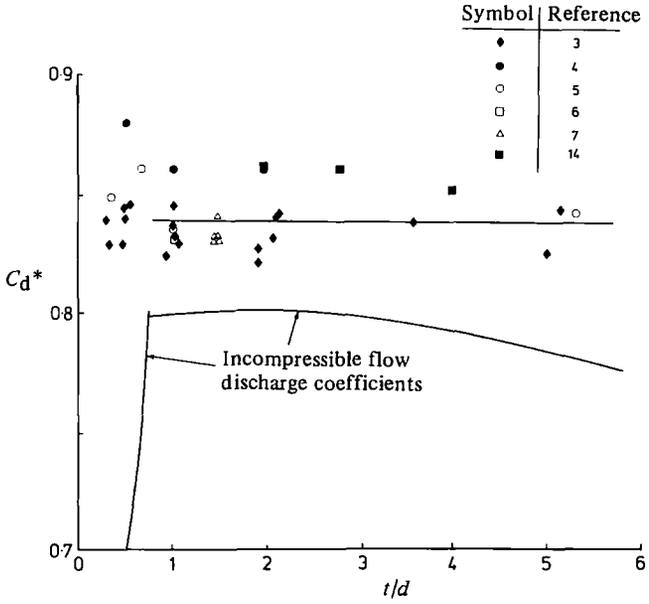

Fig. 5. Discharge coefficient as a function of t/d (Published data)

An important experimental result in the present context is the value of Cd^* reported by Jackson for $t/d = 10{\cdot}62$. This value of t/d is considerably larger than any other for which data are available and it is significant that the value of $Cd^* = 0{\cdot}82$ is lower than the remaining values quoted by the author. This evidence alone suggests that the result is for an orifice satisfying the condition $t/d > \varepsilon$. Conclusive evidence for this deduction is provided by the pressure distributions within the nozzles reported by Jackson (**5**). This particular nozzle, $t/d = 10{\cdot}62$, is clearly choking at exit, whereas all the other nozzles are choking in the plane of maximum contraction. The data of Jackson are consistent with a value for ε of about 10. In Section 2.4 a theoretical analysis is given which indicates that ε is a function of Reynolds number and surface roughness. It is not possible to make a direct theoretical prediction of the value for ε in Jackson's tests, because the range of Reynolds numbers tested have not been reported. A rough estimate can be made as follows. The devices tested by Jackson (**5**) had a relative roughness of about 0·003 for which the corresponding value of f, assuming a Reynolds number of 10^5, is 0·007. Taking $Cd^* = \phi^* = 0{\cdot}84$, we have, from Fig. 4, $\psi = 0{\cdot}353$. For $L/d \approx 11$, a value for K of 1·13 is appropriate (**13**). Hence for these conditions, if a value of $\delta = 0{\cdot}3$ is taken, we have $\varepsilon \approx 11{\cdot}5$, which compares favourably with experiment.

3.2 Some New Experimental Results

The preceding discussion has shown that the range of values of t/d of interest in the present context extend from $t/d \to 0$ to values of t/d as high as 11·5 or more. By and large it has proved possible to confirm the predictions of earlier Sections using existing experimental data. However, none of the sets of data so far discussed embraces in a single experiment the full range of values of t/d, nor covers sufficiently high values of t/d, to clearly demonstrate the effects of Fanno-choking on Cd^*. It was decided, therefore, to perform a series of tests, the principal objective of which was to examine in a consistent manner the effect of t/d on Cd^* for t/d values in the range $0{\cdot}5 < t/d < 30$. These tests formed part of a final-year undergraduate project. Conditions corresponded to the limit $\beta \to 0$.

The nozzle used in these tests was manufactured from brass and the same basic nozzle was used for all values of t/d. An initial test was made at $t/d = 29{\cdot}92$, and subsequent values of t/d were obtained by machining away the downstream face of the nozzle. In order to give priority to testing the effect of t/d and preserving consistency at the upstream face, some sacrifice was accepted in the quality of the internal bore of the nozzle. This was justifiable because the theoretical considerations of Section 2 indicated that surface roughness does not affect Cd^* in the range $\delta < t/d < \varepsilon$, which is of greatest interest. The internal finish was the unreamed bore left by a $\frac{1}{8}$ in (0·317 5 cm) long-series drill. The final dimensions of the nozzle (in cm.) are given in Fig. 6. An error analysis indicated that the absolute magnitudes of the measurements of Cd^* could be subject to uncertainties defined by a tolerance band of $\pm$ 1·6 per cent for $t/d < 10$ rising to $\pm$ 3 per cent for $t/d = 30$. The results of these tests are plotted in Figs. 7 and 8.

Although the magnitudes of Cd^* are rather lower than those reported elsewhere, Fig. 7 further confirms that there exists a substantial range of values of t/d at which Cd^* is constant. For these tests the lower bound is given by $t/d = \delta \approx 1$ and the upper bound corresponds to $t/d = \varepsilon \approx 7$. As argued previously this upper bound depends upon the Reynolds number and the relative roughness of the internal bore of the nozzle. For the present tests Re at choking varied between $0{\cdot}8 \times 10^5$ and $1{\cdot}32 \times 10^5$.

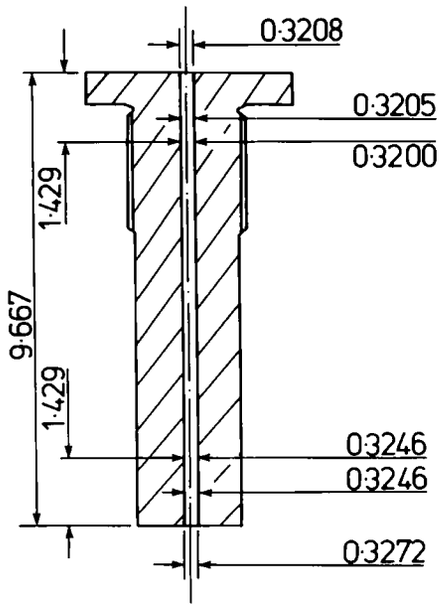

Fig. 6. Test nozzle (dimensions in cm)

4 CONCLUDING REMARKS

Theoretical and experimental evidence has been used to demonstrate that, for sharp-edged orifices, there exists a range of values of t/d, for which, within experimental limits, the critical discharge coefficient is independent of Reynolds number and t/d. This result has important practical consequences. The range is determined by the limit $\delta < t/d < \varepsilon$. Theory indicates that the magnitude of δ is determined solely by the sharpness or otherwise of the leading edge of the orifice. The actual magnitude of δ has not been precisely determined, but, for the orifices with nominally sharp edges that have been investigated, the experimental results analysed give results varying from $\delta \approx 0{\cdot}3$ to $\delta \approx 1$. Theory shows that the upper limit $t/d = \varepsilon$ is a function of Reynolds number and relative roughness. For the rough bore used in the present experiments a value of $\varepsilon = 7$ was determined; other results where a smoother bore was used are consistent with $\varepsilon \approx 10$.

Both published data (**3**, **4**, **5**, **14**) and those reported here provide substantial experimental evidence for the existence of the flow regime where Cd^* is independent of t/d. However there is less agreement on the precise magnitude of Cd^* in this regime. The variations that exist (measurements fall in the band $0{\cdot}81 < Cd^* < 0{\cdot}86$) pinpoint two factors of crucial importance if this type of device is to be employed as a practical form of critical flowmeter. Firstly slight variations in the sharpness of the leading edge undoubtedly lead to variations in Cd^*. Secondly, because the orifice diameters of interest

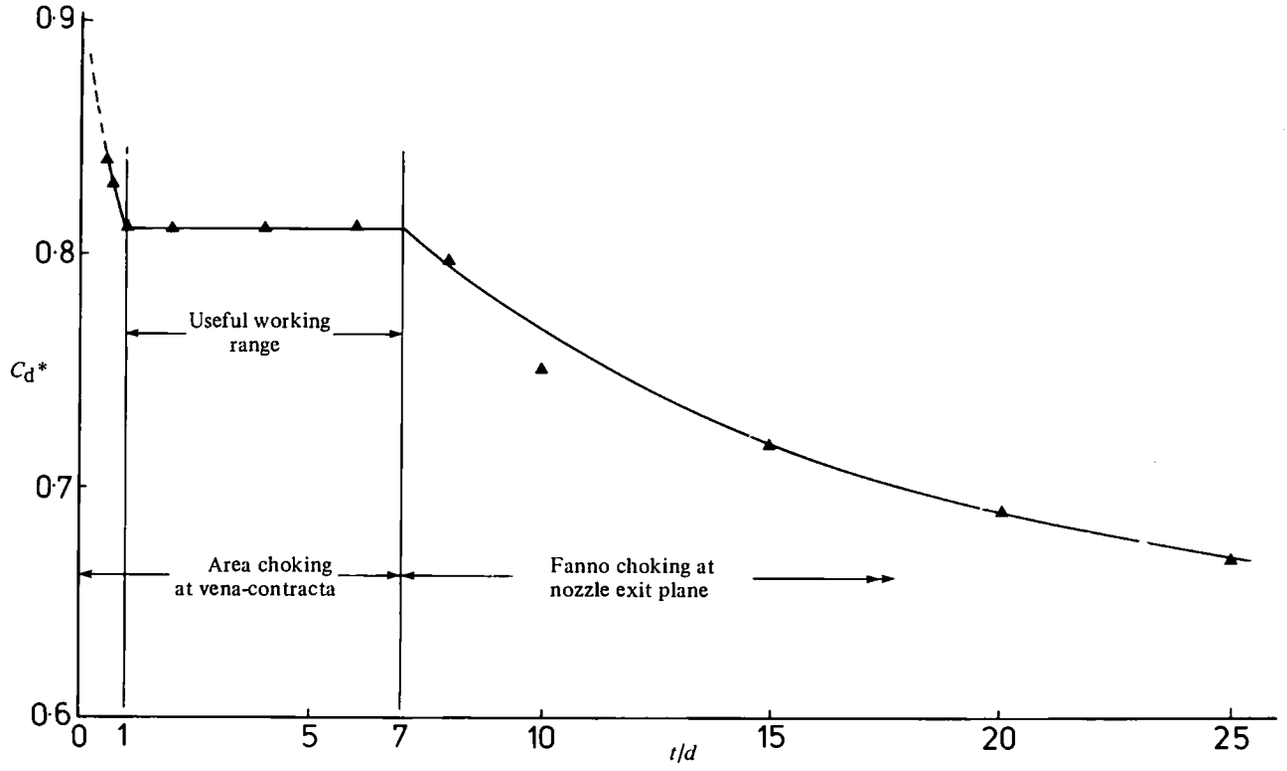

Fig. 7. Graph showing the relationship between critical discharge coefficient, Cd^*, and nozzle length to diameter ratio, t/d
▲ Present tests

are so small, even slight inaccuracies in the measurement of the internal diameter of the nozzle can lead to significant discrepancies in the estimation of mass flow rate. This second factor is of course shared by all designs of critical flowmeter, and not just those with sharp upstream edges. There is little doubt that, with care, the effects of both of these factors can be reduced to small proportions.

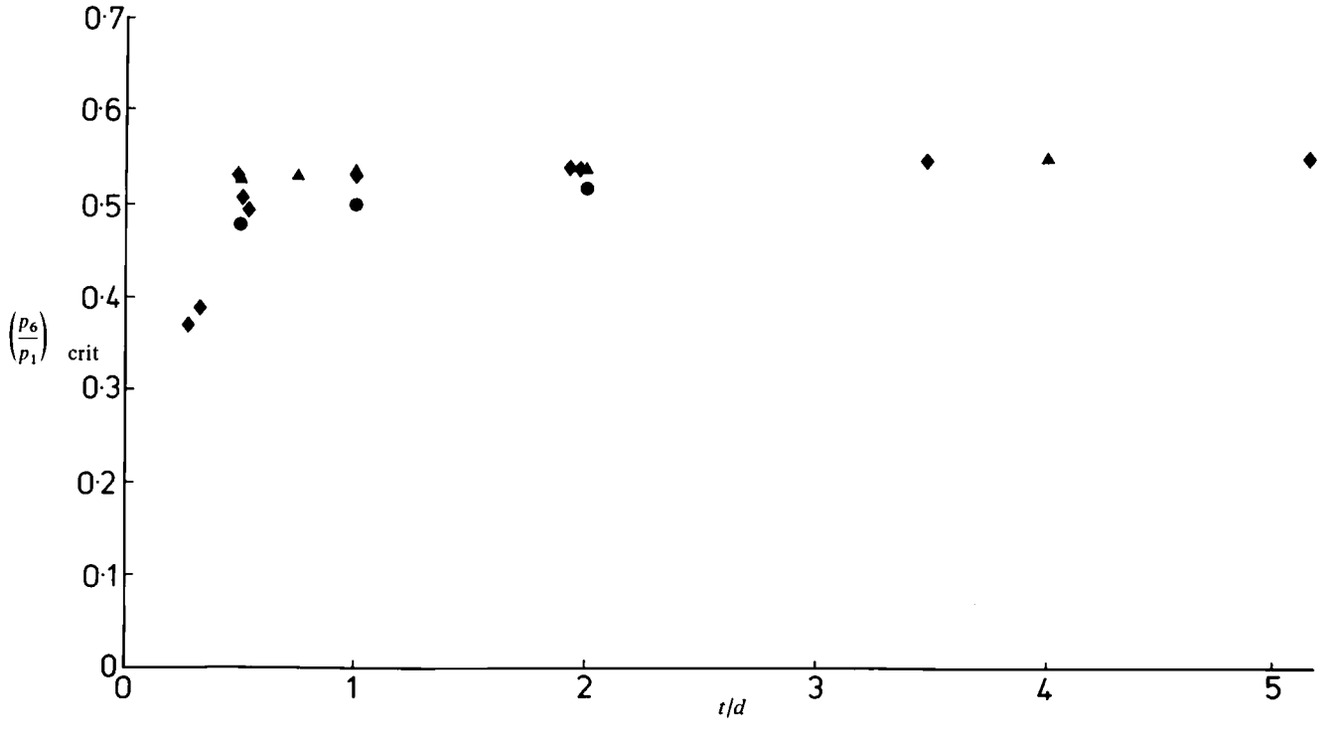

Fig. 8. Comparison of critical back pressure ratios at the onset of choking for t/d ratios in the range 0 to 5·2
◆ Brain and Reid; ● Deckker and Chang; ▲ Present tests

REFERENCES

(1) SHAPIRO, A. H. *The dynamics and thermodynamics of compressible fluid flow*. 1953 (The Ronald Press Co.)

(2) ARNBERG, B. T., BRITTON, C. L., and SEIDL, W. F. 'Discharge coefficient correlations for circular-arc venturi flowmeters at critical (sonic) flow', *Trans. Am. Soc. Mech. Engrs.*, 1974, *Series I*, **96**, 111–123

(3) BRAIN, T. J. S., and REID, J. 'Performance of small diameter cylindrical critical flow nozzles', *National Engineering Laboratory Report 546*, 1975

(4) DECKKER, B. E. L., and CHANG, Y. F. 'An investigation of steady compressible flow of air through square edged orifices', *Proc. Instn. Mech. Engrs.*, 1965–66, **180**, (Pt. 3J), 312–323

(5) JACKSON, R. A. 'The compressible discharge of air through small thick plate orifices', *Appl. Scient. Res., Section A*, 1963, **13**, 241–248

(6) GRACE, H. P., and LAPPLE, C. E. 'Discharge coefficients of small diameter orifices and flow nozzles', *Trans. Am. Soc. Mech. Engrs.*, 1951, **73**, 639–647

(7) KASTNER, L. J., WILLIAMS, T. J., and SOWDEN, R. A. 'Critical-flow nozzle meter and its application to the measurement of mass flow rate in steady and pulsating streams of gas', *J. Mech. Engng. Sci.*, 1964, **6**, (1), 88–98

(8) WARD-SMITH, A. J. *Pressure losses in ducted flows*. Part 4: 'A unified treatment of the flow and pressure drop characteristics of constrictions having orifices with sharp edges', 1971 (Butterworths, London)

(9) WEIR, A., YORK, J. L., and MORRISON, R. B. 'Two and three-dimensional flow of air through square-edged sonic orifices', *Trans. Am. Soc. Mech. Engrs.*, 1956, **78**, 481–488

(10) STANTON, T. E. 'On the flow of gases at high speeds', *Proc. R. Soc.*, 1926, **111**, 306

(11) BRAGG, S. L. 'Effect of compressibility on the discharge coefficient of orifices and convergent nozzles', *J. Mech. Engng Sci.*, 1960, **2**, 35–44

(12) JOBSON, D. A. 'Flow of a compressible fluid through orifices', *Proc. Instn. Mech. Engrs.*, 1955, **169**, 37

(13) BARBIN, A. R., and JONES, J. B. 'Turbulent flow in the inlet region of a smooth pipe', *Trans. Am. Soc. Mech. Engrs., Series D*, 1963, **85**, (1), 29–34

(14) ROHDE, J. E., RICHARDS, H. T., and METGER, G. W. 'Discharge coefficients for thick plate orifices with approach flow perpendicular and inclined to the orifice axis', *National Aeronautics and Space Administration NASA TN D-5467*, 1969

(15) BENSON, R. S., and POOLE, D. E. 'Compressible flow through a two-dimensional slit', *Int. J. Mech. Sci.*, 1965, **7**, 315–336

(16) BENSON, R. S., and POOLE, D. E. 'The compressible flow discharge coefficients for a two-dimensional slit', *Int. J. Mech. Sci.*, 1965, **7**, 337–353

ACKNOWLEDGEMENT

The contributions of P. J. Dunford, who was involved in the development of the theoretical methods discussed here, and J. W. Thompson, whose experimental results are quoted in Section 3.2, are acknowledged with gratitude.